To be published in "Construction and Building Materials"
Received at Editorial Office: 22 Feb 2017
Article revised: 17 Apr 2017
Article accepted for publication: 18 Apr 2017
DOI10.1016/j.conbuildmat.2017.04.166

Mechanical properties, drying shrinkage, and creep of concrete containing lithium slag

Zhi-hai He[1], Long-yuan Li[2*], Shi-gui Du[1*]

1) College of Civil Engineering, Shaoxing University, Shaoxing 312000, China

2) School of Engineering, University of Plymouth, PL4 8AA, UK

*) Corresponding authors (dsg@usx.edu.cn)

Abstract - This paper presents an experimental study on the compressive strength, elastic modulus, drying shrinkage, and creep of concrete added with lithium slag as a supplementary cementitious material. The effects of the lithium slag on these mechanical properties were examined experimentally by using specimens with different lithium slag contents (0%, 10%, 20% and 30% of binder). In addition, mercury intrusion porosimetry and scanning electron microscope techniques were also used to investigate the pore microstructure of the concretes with different lithium slag contents to support the findings obtained from the mechanical property tests. It was shown that, the addition of lithium slag in concrete can improve the mechanical properties of matured concrete, including the compressive strength, elastic modulus, drying shrinkage and creep, if the right amount of lithium slag is used.

Keywords: Concrete, compressive strength, creep, lithium slag, supplementary cementitious material.

1. Introduction

Efforts have been made in recent decades to develop “green” concretes containing industrial waste [1-4]. It is well known that in such green concretes cement has been partially replaced by industrial and/or agricultural byproducts such as fly ash, ground granulated blast furnace slag, metakaolin, rice husk ash, etc., which are considered as supplementary cementitious materials (SCMs). The replacement of cement by using SCMs not only decreases the landfills of waste materials and their associated environmental impacts, but also reduces the carbon footprint of concrete. In general, SCMs can be used to improve the mechanical properties of concrete, either in fresh or hardened mixtures [5-8]. In addition, using SCMs can also decrease the cost of construction while providing “green” concrete with comparable mechanical properties. Therefore, SCMs are widely used in concrete either in blended cement or added separately in concrete mixtures [9-11]. The continuously increasing demand of SCMs used in concrete results in the great shortage of traditional SCMs. Therefore, there is a need to find new types of SCMs which can be used in concrete.

In China, a great amount of lithium slag (LS) is discharged as a byproduct in the process of the lithium carbonate using sulfuric acid method when the spodumene ore is calcined at high temperature of 1200 ^{o}C. The main formation process of LS is shown in Fig.1.

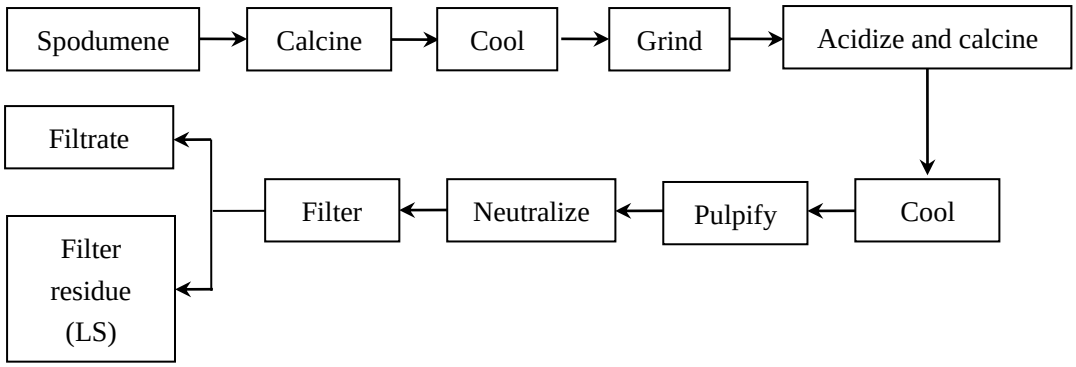

Fig.1 Formation process of LS

According to the statistical analysis [12], about nine tons of LS are discharged when

one ton lithium salt is produced in the production process of lithium carbonate. Today, about $8x10^5$ tons of LS are discharged every year in China. The disposal of such large quantities of LS not only results in the shortage of landfills but also causes serious environmental pollution problem. Therefore an urgent task is to find an efficient way to recycle the disposed LS. Considering the grindability and certain pozzolanic reactivity because of the high content of active silicon dioxide and aluminium oxide, LS may be used as a SCM in cement and concrete. However, from a literature survey there are very limited references on the use of LS in concrete [13-15], and the effect of LS on the mechanical properties of concrete such as drying shrinkage and creep has not been discussed.

In this paper, an experimental study on the mechanical properties, drying shrinkage, and creep of concrete containing LS as a SCM is presented. The effects of LS on the compressive strength, elastic modulus, drying shrinkage, and creep of the concrete containing LS were examined using an experimental method. The mercury intrusion porosimetry (MIP) and scanning electron microscope (SEM) techniques were also used to investigate the pore microstructure of the mixed concrete to support the findings obtained from the experiments.

2. Experimental

2.1 Materials

The cement used in the present study was ordinary Portland cement of Grade P·O42.5 according to common Portland cement (Chinese GB 175-2007). The LS used was supplied by Sichuan lithium salt plant in China, whose appearance is shown in Fig.2. It can be seen from the figure that the appearance of LS is earthy yellow.

Fig.2 Appearance of LS

Table 1 gives the chemical properties of the cement and LS used, which shows that the LS has far more SiO_2 and Al_2O_3, but much less CaO than the cement does. In addition, the content of SO_3 of the LS is also more than that of the cement.

Table 1 Chemical compositions of cement and LS (wt %)

Materials	SO_3	SiO_2	Fe_2O_3	Al_2O_3	CaO	MgO	K_2O	Na_2O	Loss on ignition
Cement	2.42	20.34	3.43	4.76	61.87	1.34	0.55	0.06	3.11
LS	7.15	53.22	1.48	17.11	10.11	0.41	0.53	0.33	8.25

The particle size distributions of the cement and LS were determined by laser particle analysis using BT-9300 Laser Particle Analyzer, which are shown in Fig.3. It can be seen from the figure that the size range of LS particles is narrower than that of cement particles. However, in terms of the average size, LS particle is smaller than cement

particle, which is demonstrated in the grading curves of cement and LS shown in Fig.4.

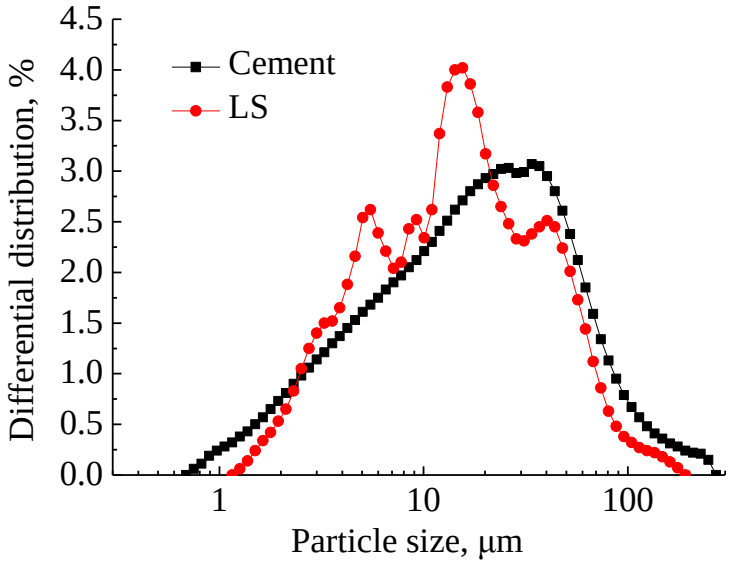

Fig.3 Particle size distributions of cement and LS

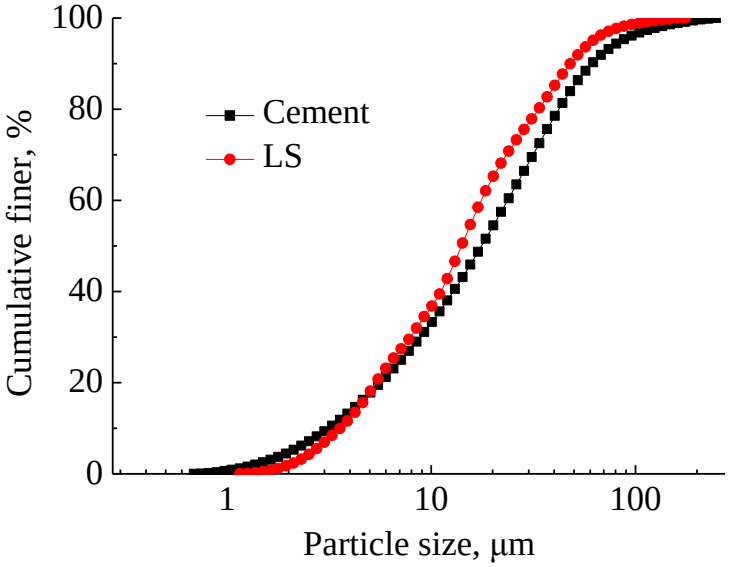

Fig.4 Grading curves of cement and LS

The specific gravities of cement and LS are about 2910 and 2450 kg/m^3, respectively,

which were determined according to the standard test method for cement density (Chinese GB/T208-2014) using the small pycnometer method. The specific surface area is about 360 m^2/kg for cement and 440 m^2/kg for LS, respectively, which were determined based on the nitrogen adsorption method. In addition, LS particles were found to be irregular in shape, which can be demonstrated in the SEM image shown in Fig.5.

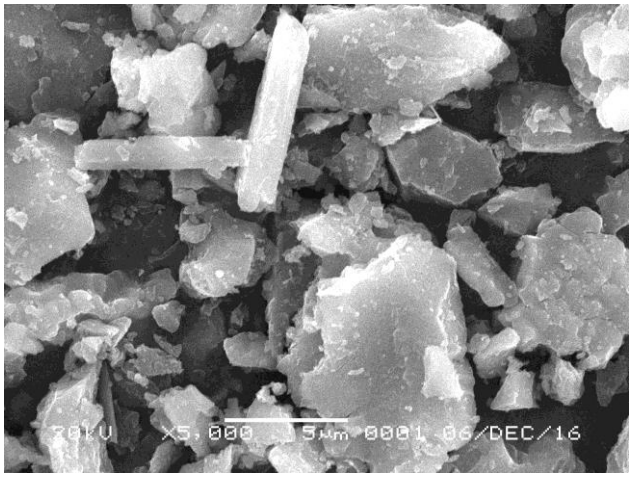

Fig.5 SEM image of LS

River sand was used for fine aggregates, which has a fineness modulus of 2.5 and a specific gravity of 2550 kg/m^3. Crushed limestone was used for coarse aggregates, which has a size range from 5.0 mm to 25 mm, and a specific gravity of 2660 kg/m^3. The specific gravity and the sieve analysis for both fine and coarse aggregates were done as specified in the standard for technical requirements and test method of sand and crushed stone (or gravel) for ordinary concrete (Chinese JGJ 52-2006). The polycarboxylic superplasticizer admixture with a specific gravity of 1200 kg/m^3 was

used, which allows a water reduction up to 25%.

2.2 The concrete mixture proportioning

Mixture proportioning was carried out according to specification for mix proportion design of ordinary concrete (Chinese JGJ 55-2011). The targeted compressive strength was 50 MPa for the control mixture.

Four types of concrete mixtures of different LS contents (0%, 10%, 20% and 30% of binder) were used in the experiments. In all types of mixtures the binder to aggregate ratio, fine aggregate to aggregate ratio, and water to binder ratio were kept as constants, which are 0.25, 0.41, and 0.35, respectively. The superplasticizer content was adjusted to maintain a slump of 150-180mm for all mixtures. Table 2 shows the details of the relative weight of each component used in each type of mixtures.

Table 2 Mix proportions of concretes with different LS (in weight)

Types of mixture	Cement	LS	River sand	Crushed limestone	Water	Superplasticizer
C	450	0	735	1055	158	3.83
C+10LS	405	45	735	1055	158	4.23
C+20LS	360	90	735	1055	158	4.47
C+30LS	315	135	735	1055	158	4.58

2.3 Test methods

Four groups of specimens were casted for each mixture. One is for the compressive

strength test, in which the dimensions of the specimens are 150 mm x 150 mm x 150 mm. One is for the elastic modulus test, in which the dimensions of the specimens are 150 mm x 150 mm x 300 mm. One is for the drying shrinkage test, in which the dimensions of the specimens are 100 mm x 100 mm x 300 mm. One is for the creep test, in which the dimensions of the specimens are same with those in the drying shrinkage test.

For the compressive strength and elastic modulus tests, after mixing and casting, the specimens were kept in moulds for about 24 hours at room temperature (20±5) ^{o}C. After that, they were demoulded and placed in a standard curing room of controlled temperature (20±2) ^{o}C and relative humidity more than 95% for 27 day curing before they were tested (that is a total of 28 days from mixing to testing). Both the compressive strength and elastic modulus tests were carried out using Instron testing machine, by following the standard for test method of mechanical properties on ordinary concrete (Chinese GB/T 50081-2002).

The drying shrinkage and creep tests were carried out simultaneously. After mixing and casting, specimens were kept in moulds for about 24 hours at room temperature (20±5) ^{o}C. After that, they were demoulded and placed in a standard curing room of controlled temperature (20±2) ^{o}C and relative humidity more than 95% for another 6 days (that is a total of 7 days from mixing to testing) before they were tested in drying shrinkage and creep testing machine. During the drying shrinkage and creep tests the

temperature and relative humidity were controlled at about (20±2) ^{o}C and (60±5) %, respectively.

For the creep test, a constant load, corresponding to 25% of the cubic compressive strength of the specimen obtained at 7days, was applied along the axial direction of the specimens by compressing the spring. Note that the use of 7 days instead of 28 days compressive strength is because in practice load can be applied when a concrete has cured for 7 days although its strength is lower than that at 28 days. When the specimens were being loaded, four dial indicators placed along the tested specimens were used to indicate the loading direction and to ensure the loading was applied along the axial direction of the specimens. The creep under the constant load was monitored by the dial indicators. Note that the strain recorded from the dial indicators involves not only the creep strain but also the drying shrinkage strain. In order to eliminate the drying shrinkage strain, a separate test of the specimen without loading was carried out for each tested specimen, from which the drying shrinkage strain was obtained. The creep strain thus was calculated from the difference between the strains obtained from the creep and shrinkage tests. Since both tests were carried out for specimens after the 7 days curing the autogenous shrinkage was ignored in both the creep strain and drying shrinkage strain obtained from the tests. The processes of drying shrinkage and creep tests are shown in Fig.6 and Fig.7, respectively. Table 3 summarizes the tests carried out for the four groups of specimens.

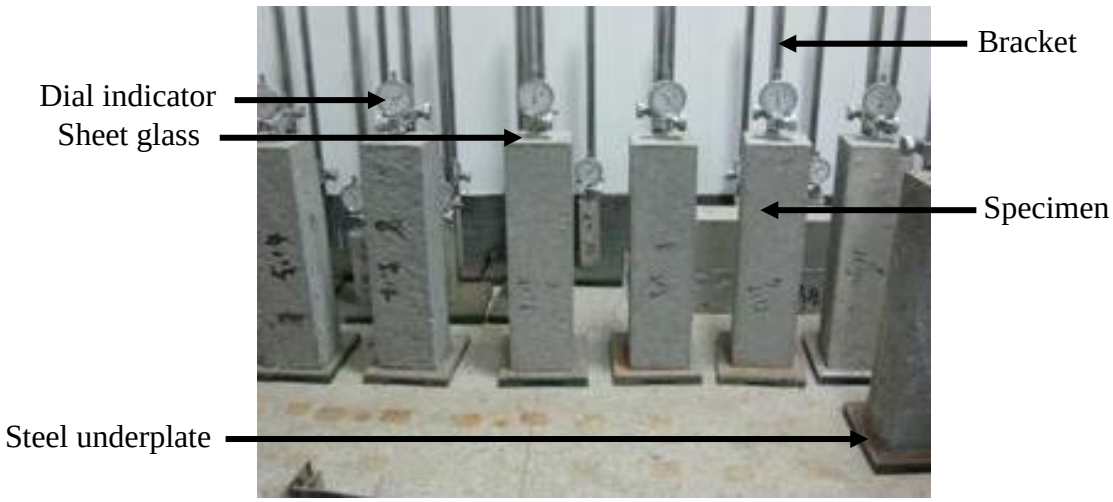

Fig.6 Processes of drying shrinkage test

Fig.7 Processes of creep test

Table 3 Summary of tests

Type of tests	Specimen dimensions (mm)	Age of specimens before test (days)	No of specimens tested*
Compressive strength	150x150x150	7, 28, 60 and 90	4x3x4

Elastic modulus	150x150x300	7, 28, 60 and 90	4x6x4
Creep	100x100x300	7	2x2x4
Drying shrinkage	100x100x300	7	3x4

Note*: 4 is the types of concrete mixtures

MIP and SEM techniques were used to measure the pore size and its distribution and to examine the pore microstructure in hardened concrete specimens containing LS (normally 7 days and 90 days). The specimens used for the MIP and SEM tests were first broken into small pieces of size 3-5 mm, which consist of only mortar and fine aggregates, and then stored in ethanol solution for 3 days to prevent further hydration and/or carbonation. After then, they were dried and stored in sealed containers before the MIP and/or SEM tests were carried out.

3. Results and discussions

3.1 Compressive strength and elastic modulus

Compressive strength was obtained by using pure uniaxial compression. The cubic compressive strength was calculated by using the maximum load divided by the original cross-section area of the specimen. Fig.8 shows the variation of the compressive strength with the LS content added in the concrete mixture at the different testing time. Each result presented here is the average value of three tested specimens with identical mixture, and the error bar represents the variation of the obtained data.

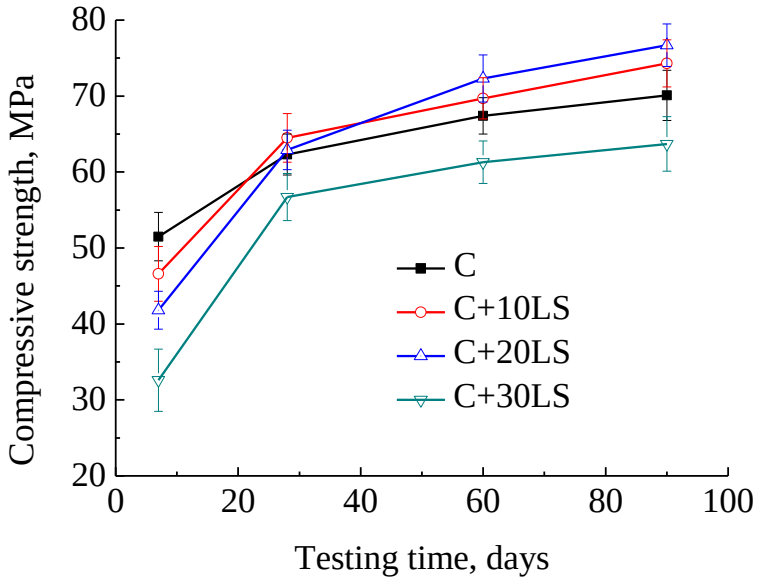

Fig.8 Effect of LS on compressive strength of specimens (error bar represents the variation of test data).

It is seen from the figure that LS has an obvious effect on the compressive strength development of the specimens. The results indicate that the more LS is added, the lower the compressive strength is attained at the early age (7 days). However, from the start of 28 days, the compressive strengths of specimens containing 10% or 20% LS are higher than that of the control specimen without LS. The specimen containing 20% LS shows the highest compressive strength at the later age (60 and 90 days). However, the compressive strength of the specimen containing 30% LS is the lowest for all the time. This may be attributed to the fact that the pozzolanic reaction of LS is slow, which depends mainly on the availability of calcium hydroxide (CH). It is well known that CH is produced by the hydration of Portland cement and consumed by the pozzolanic reaction. When the content of cement is too few, or the content of LS is too many (30%), only few CH is produced which cannot effectively stimulate the

pozzolanic reaction of LS. In this situation, LS shows mainly the physical fill effect to decrease the compressive strength. Wu et al. [16] reported that the later compressive strength of specimens produced by high early strength cement were not decreased for the mix with less than 20% LS and the optimum compressive strength for water to binder ratio of 0.35 was the mix with 15% LS substitution. However, Zhang [17] found that the compressive strengths of specimens produced by high early strength cement at 28 days were not decreased with the percentage of LS up to 40% replacement for water to binder ratio of 0.28, and the highest compressive strength corresponded to the mix containing 15% LS. These results indicate that the effect of LS on the compressive strength depends mainly on the water to binder ratio, the type of cement and the percentage of LS used in the binder.

The modulus of elasticity of the specimen was determined by centering and prepressing the specimens. The loading schematic diagram of elastic modulus test is shown in Fig.9.

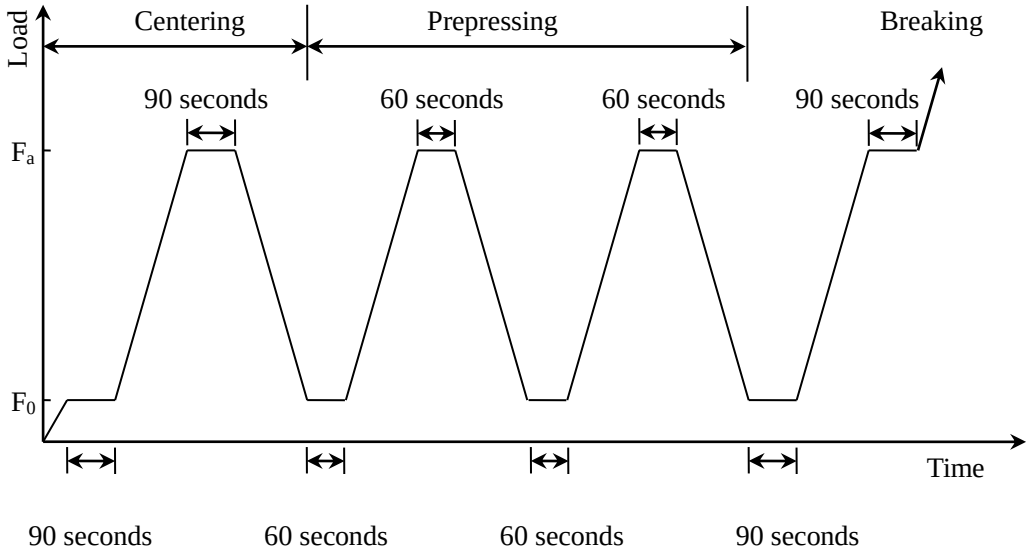

Fig.9 Loading schematic diagram of elastic modulus test

The elastic modulus can be calculated as follows:

$$E = \frac{F_a - F_0}{A} \times \frac{L}{\Delta n} \quad (1)$$

$$\Delta n = \varepsilon_a - \varepsilon_0 \quad (2)$$

where E in MPa is the elastic modulus, F_a in N is the load corresponding to the stress which is 1/3 of axial compressive strength, F_0 in N is the initial load corresponding to the stress which is 0.5MPa, A in mm^2 is the bearing pressure area, L in mm is the test gauge length, Δn in mm is the average deformation value of two sides of the specimen when the load from F_0 up to F_a in the last time, ε_a in mm is the average deformation value of two sides of the specimen when the load is F_a, ε_0 in mm is the average deformation value of two sides of the specimen when the load is F_0.

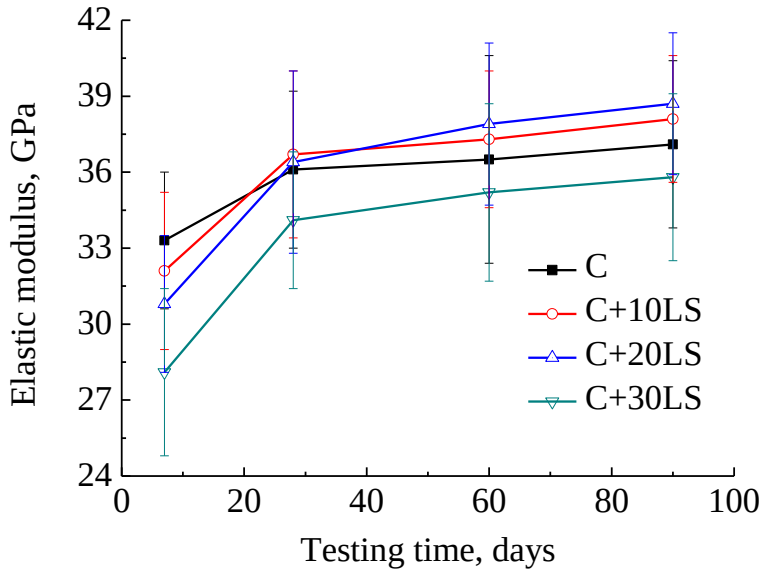

Fig.10 Effect of LS on elastic modulus of specimens (error bar represents the variation of test data).

Fig.10 shows the variation of the elastic modulus with the LS content added in the

concrete mixture at the different testing time. Similarly to the compressive strength, the data shown here is the average value of three tested specimens with identical mixture, and the error bar represents the variation of the obtained data. It can be seen from the figure that the variation of the elastic modulus with the LS is very similar to that of the compressive strength at the different testing time. When cement is replaced by LS equivalently, the content of the paste of unit concrete with LS is more than that of unit control concrete without LS, because the specific gravity of LS is lower than that of cement. The excessive content of paste is adverse to increase the elastic modulus of concrete.

Kim et al. [18] reported that there was a linear relationship between the elastic modulus and the quadratic root of compressive strength of ordinary concrete. To identify the correlation between the elastic modulus and compressive strength of the concrete containing LS at different testing times, Fig.11 plots the relationship between the elastic modulus and the quadratic root of compressive strength obtained from the test at different testing times.

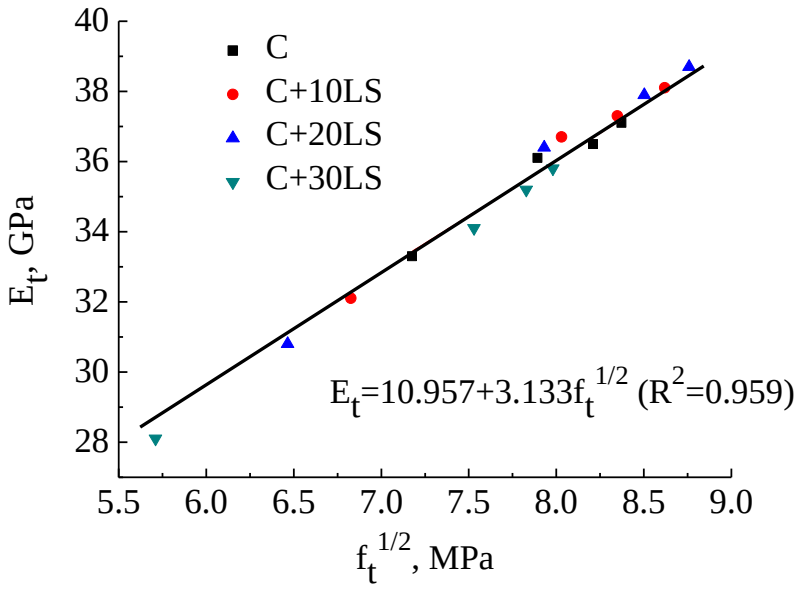

Fig.11 Relationships between elastic modulus and quadratic root of compressive strength (E_t is the elastic modulus at t days, $f_t^{1/2}$ is the quadratic root of compressive strength at t days)

It can be seen from the figure that there is also a linear relationship between the elastic modulus and the quadratic root of compressive strength of concrete containing LS, which corresponds well with the results reported by Kim et al. [18]. In addition, with the increase of concrete age, the increasing rate of compressive strength is greater than that of the elastic modulus.

3.2 Drying shrinkage

After 7 days for mixing, casting and curing, the test of drying shrinkage is carried out. Fig.12 shows the drying shrinkage strain of the specimens with different LS-to-binder ratios at different testing times. Each result is the average value obtained from 3 tested

specimens with identical mixture, whereas the error bars show the variation of the obtained data. It can be observed from the figure that, all of the specimens exhibit a similar variation trend, in which the drying shrinkage strain increases quickly for the first 60 days, but after then the increasing rate becomes very slow and tends to be stable. LS can effectively decrease the drying shrinkage strain, but the effect of the content of LS on the drying shrinkage strain seems unequally. For example, adding 10%, 20% and 30% LS in binder decreases drying shrinkage strain at 180 days since the testing by 16%, 27% and 21%, respectively. This indicates that there is an up-limited effect of LS on the drying shrinkage strain and of the three mixtures 20% LS seems to be the best in terms of the decrease of the drying shrinkage strain.

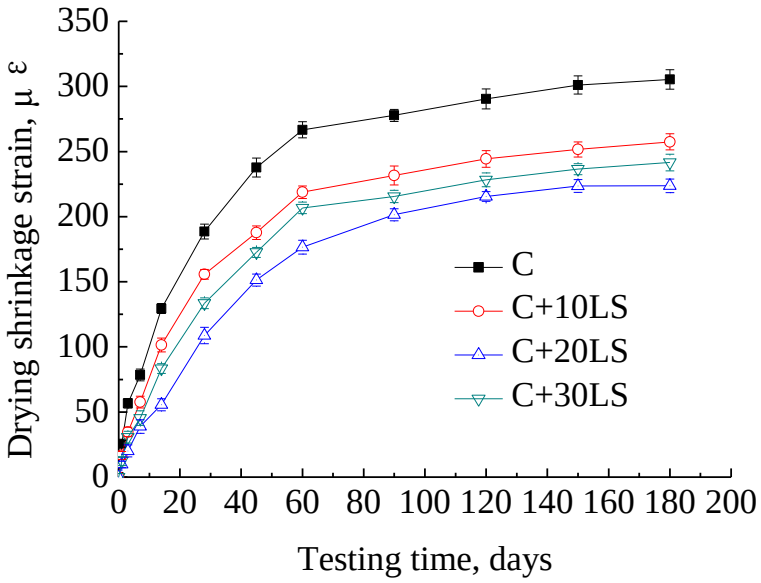

Fig.12 Effect of LS on drying shrinkage strain of specimens (error bar represents the variation of test data).

3.3 Creep

The test of creep was carried out simultaneously with the test of the drying shrinkage. The creep strain was calculated by using the strain obtained from the creep test subtracting the corresponding drying shrinkage strain obtained in a separate test as described in the above section. Fig.13 shows the creep strain of the specimens with different LS-to-binder ratios at different loading times. Each result is the average value obtained from 2x2 tested specimens with identical mixture, whereas the error bars show the variation of the obtained data.

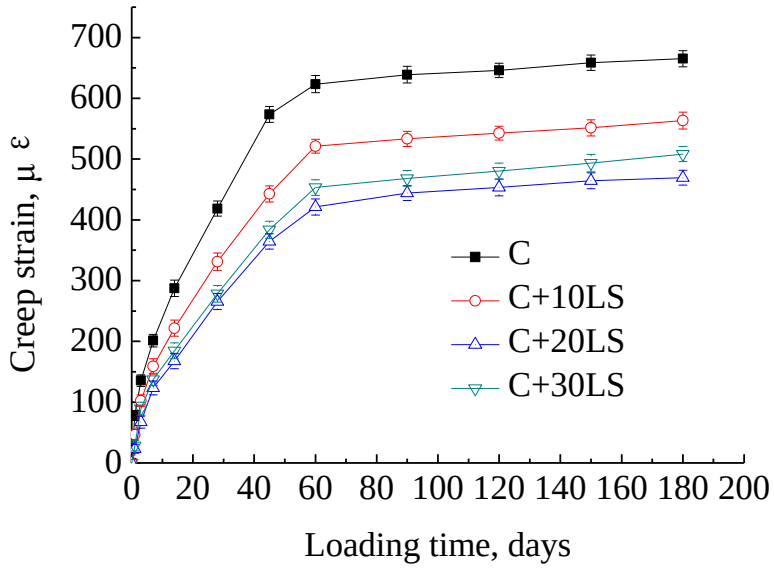

Fig.13 Effect of LS on creep strain of specimens (error bar represents the variation of test data).

It appears that for each mixture the creep strain and drying shrinkage strain have similar tendency, although in terms of the value the creep strain is more than twice of the drying shrinkage strain. The effect of LS on the creep strain is also similar with

that of LS on the drying shrinkage strain. For example, adding 10%, 20% and 30% LS in binder decreases the creep strain at 180 days since the loading by 15%, 29% and 24%, respectively. This also indicates that of the three mixtures 20% LS seems to be the best in terms of the decrease of the creep strain. Note that the creep strain shown in Fig.13 was obtained from the compressive tests with constant axial stresses. To eliminate the effect of stress scale on the creep, one usually uses the creep coefficient or the specific creep. The former is defined as the ratio of the creep strain to the elastic strain as follows,

$$C_{cc} = \frac{\varepsilon_{cs}}{\varepsilon_{es}} = \frac{\varepsilon_{cs}}{\sigma / E_7} = \frac{4\varepsilon_{cs}}{f_7 / E_7} \tag{3}$$

where C_{cc} is the creep coefficient, ε_{cs} is the creep strain, ε_{es} is the elastic strain, σ is the applied compressive stress ($\sigma = 0.25 f_7$ in the present experiments), f_7 is the cubic compressive strength of the specimen at 7days, E_7 is the elastic modulus at 7 days. Using Eq.(3), the four curves shown in Fig.13 can be re-plotted as the curves of creep coefficient versus the loading time, which are shown in Fig.14.

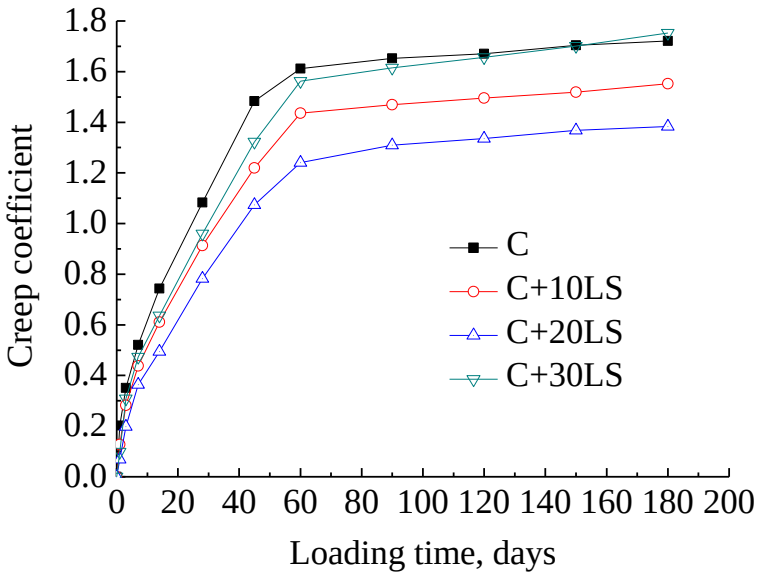

Fig.14 Effect of LS on creep coefficient of specimens

It can be seen from the figure that the variation of creep coefficient with the loading time is different from that of the creep strain with the loading time shown in Fig.13. For example, adding 10% and 20% LS in binder decreases creep coefficient at 180 days since the loading by 10% and 20%, respectively. However, adding 30% LS in binder decreases slightly the creep coefficient at early days and increases creep coefficient at 180 days since the loading by 2%. This phenomenon may be attributed to the fact that the different variation of compressive strength shown in Fig.8 and elastic modulus shown in Fig.10 of specimens at 7 days.

The specific creep is defined as the ratio of the creep strain to the applied compressive stress. Since in each type of the mixes the applied stress is constant, Fig.13 can be re-plotted as the curves of specific creep versus the loading time, which are shown in

Fig.15. It can be seen from the figure that, adding 10% and 20% LS in binder decreases the specific creep but adding 30% LS in binder increases the specific creep. The variation feature of the three specific creep curves with LS to the loading time shown in Fig.15 seems to be similar to that of creep coefficient curves shown in Fig.14.

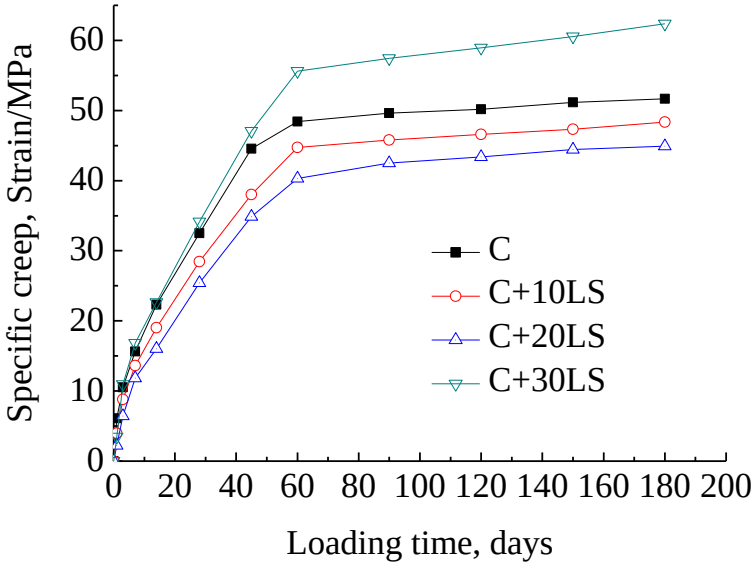

Fig.15 Effect of LS on specific creep of specimens

3.4 Pore microstructure analysis

It is well known that the cement paste formed by the hydration reactions contains interconnected pores of different sizes, namely the gel pores (a few fractions of a nm to several nm) within C-S-H, capillary pores (tens of nm to several μm), and air voids (greater than tens of μm). The SEM images with 5000 magnifications taken from samples in the specimens with different LS-to-binder ratios at 7 days and 90 days curing are shown in Fig.16 and Fig.17, respectively. It can be observed from these

images in Fig.16 that, in the control sample without LS small capillary pores exist at the early ages. In contrast, in the samples with LS the sizes of capillary pores are relatively large. The higher the LS added in the binder, the larger the sizes of capillary pores. In addition, a number of smooth particles of LS can also be found in the samples containing LS, which still remain unreacted and acted mainly as filling effect. This indicates that the addition of LS in concrete increases the porosity of the capillary pores of concrete and thus degrades the mechanical properties of the material at the early ages, as demonstrated in Fig.8 and Fig.10. Observing the later images shown in Fig.17, it can be seen that, compared to the samples at the early ages, the microstructures of samples are much denser. In the control sample without LS capillary pores still exist at the later ages. In contrast, there are very small capillary pores in the samples containing 10% and 20% LS, which are surrounded and/or filled by C-S-H gel pores produced by cement hydration and secondary pozzolanic reaction of LS. The hydration products growing from the cement particles and LS particles are to be connected. The higher the LS added in the binder, the smaller the sizes of capillary pores. However, a number of large capillary pores and smooth particles of LS can still be found in the sample containing 30% LS, indicating that some LS particles still remain unreacted. This may also explain why the variation of the properties of the specimens at the later ages.

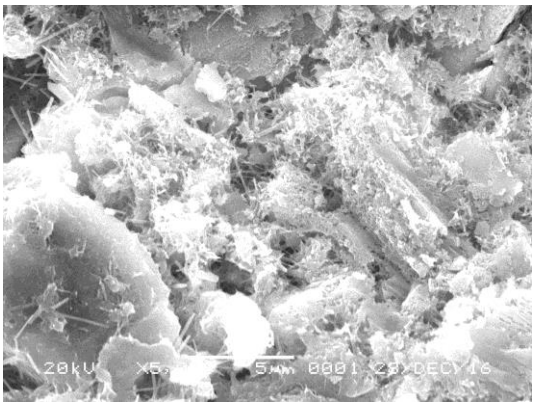

(a) Sample C

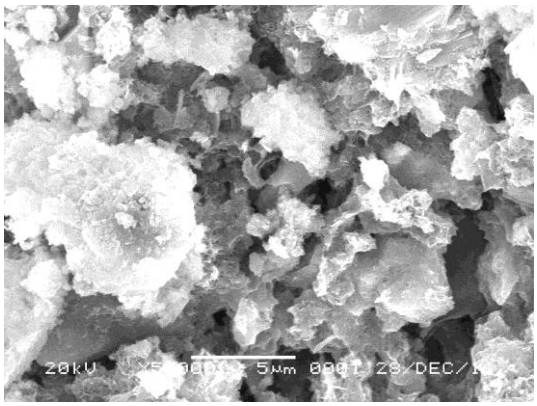

(b) Sample (C+10LS)

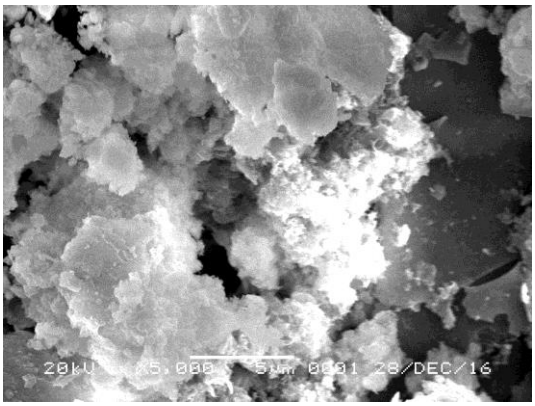

(c) Sample (C+20LS)

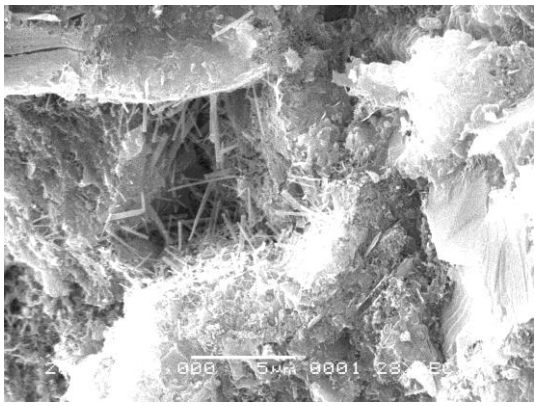

(d) Sample (C+30LS)

Fig.16 SEM images of specimens containing LS at 7 days

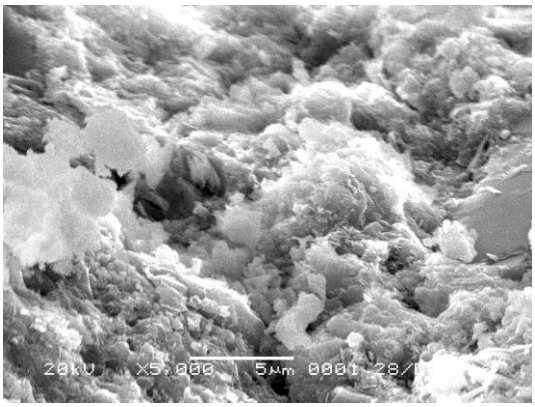

(a) Sample C

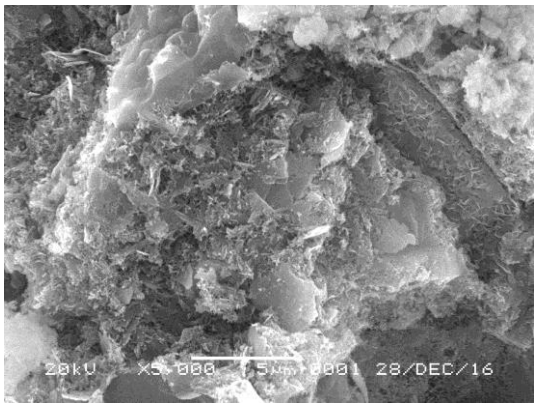

(b) Sample (C+10LS)

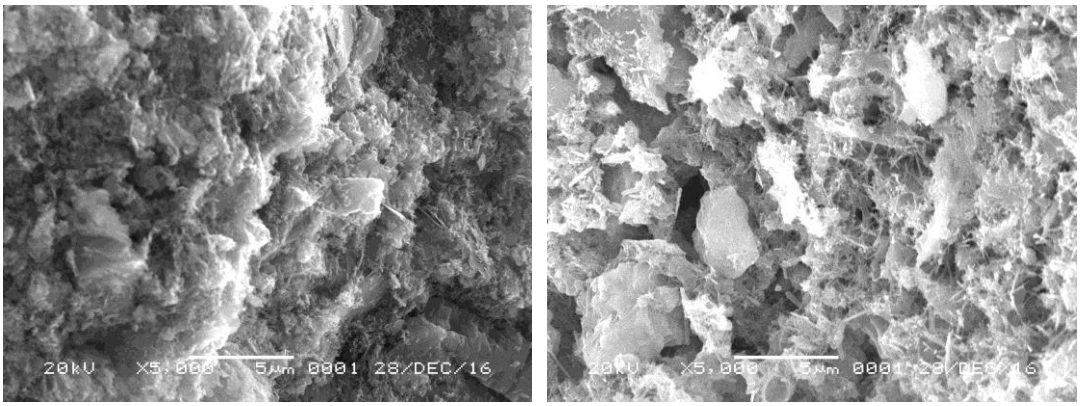

(c) Sample (C+20LS) (d) Sample (C+30LS)

Fig.17 SEM images of specimens containing LS at 90 days

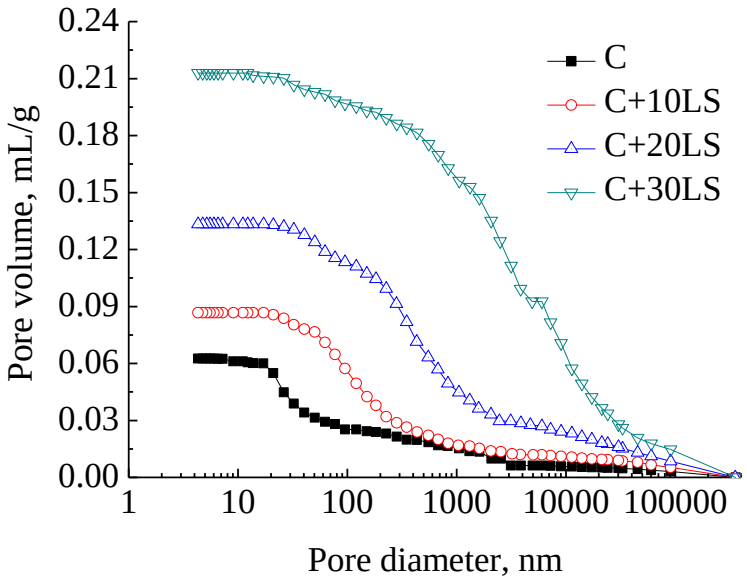

Fig.18 Effect of LS on cumulative porosity of specimens at 7 days

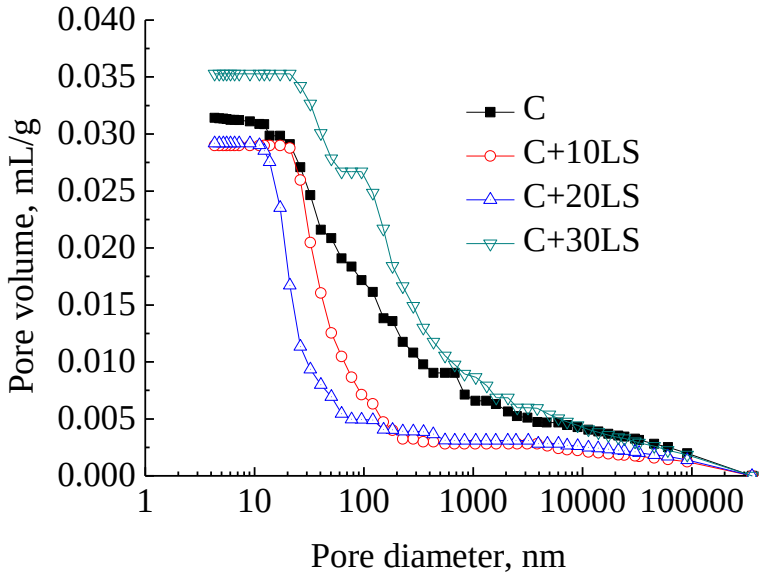

Fig.19 Effect of LS on cumulative porosity of specimens at 90 days

The average size of LS particles is much smaller than that of cement particles as it is demonstrated in Fig.3 and Fig.4. When they are mixed with cement, many small particles can fill the capillary pores of the cement paste. In addition, LS particles are also highly reactive at the later ages. They react with calcium hydroxide originated from cement hydration to produce additional C-S-H. In addition, LS particles with high content of SO_3 also generate the inflatable ettringite (AFt) in alkaline environment [15,16], which is different from other SCMs [5,19-22]. This additional C-S-H and AFt can also fill large pores and/or voids. This is why the addition of LS in concrete can reduce the creep of the mixed concrete. Fig.18 and Fig.19 show the effect of LS on the pore-size distribution at 7 days and 90 days, measured by MIP, respectively. Note that MIP is a useful tool and can serve as comparative indices for the connectivity and capacity of the pore systems in hydrated cements although it is not accurate in terms of the measures of the actual pore sizes present [23,24].

Nevertheless, the comparison of Fig.18 and Fig.19 shows that LS has an obvious effect on cumulative porosity of samples. The increase of ages leads to a decrease in pore size and/or in pore volume. Table 4 and Table 5 provide the detailed comparison of porosities of different size groups at 7days and 90 days, respectively. It is evident that the addition of LS in concrete increases the porosity of large pores at the early ages. The addition of 10% and 20% LS in binder can refine the pore structure of samples at the later ages, and however, adding 30% LS in binder increases the porosity of large pores from 7 days to 90 days. These results are corresponding well with the results shown in SEM images.

Table 4 Distribution of pore size in samples with different LS at 7 days (mL/g)

Number	<50nm	(50～100)nm	>100nm	Total porosity
C	0.031	0.008	0.024	0.063
C+10LS	0.011	0.023	0.053	0.087
C+20LS	0.009	0.013	0.111	0.133
C+30LS	0.01	0.005	0.198	0.213

Table 5 Distribution of pore size in samples with different LS at 90 days (mL/g)

Number	<50nm	(50～100)nm	>100nm	Total porosity
C	0.011	0.003	0.017	0.031
C+10LS	0.016	0.006	0.007	0.029
C+20LS	0.022	0.002	0.005	0.029
C+30LS	0.007	0.001	0.027	0.035

4. Conclusions

This paper has reported the experimental data of the compressive strength, modulus of elasticity, drying shrinkage, and creep of concrete with LS as a SCM. In addition, the pore microstructure has been analysed to examine the effect of LS on the pore size distribution and pore volume of the hardened concrete. From the present study the following conclusions can be drawn:

- The addition of LS in concrete decreases the compressive strength at the early age, but the addition of 10% or 20% LS can improve the compressive strength at the later age, and the addition of beyond 20% degrades the compressive strength for all the time.
- The effect of LS on the elastic modulus is similar to its effect on the compressive strength. There is a linear relationship between the elastic modulus and the quadratic root of compressive strength of concrete containing LS at different testing times.
- Drying shrinkage strain in concrete with LS increases quickly for the first 60 days, but after then tends to be stable. The addition of LS in concrete can decrease the drying shrinkage. Of the present three mixtures with different levels of LS the 20% LS seems to be the best in terms of the decrease of the drying shrinkage strain.
- The effect of LS on the creep strain seems to be very similar to its effect on drying shrinkage strain, except for the case where the addition of 30% LS increases slightly the creep coefficient.

- The effect of LS on the specific creep is slightly different from that of it on creep strain. Adding 10% and 20% LS in binder decreases the specific creep but adding 30% LS in binder increases the specific creep.
- As reported in literature, LS can react with cement hydration products to produce C-S-H and AFt, which can fill capillary pores and/or voids in concrete. However, too much LS content would have negative effect on concrete pore structure because the pozzolanic reaction of LS cannot be effectively stimulated.

Acknowledgments - The authors would like to acknowledge the National Natural Science Foundation of China (Grant No. 41427802 and 51602198) and the Shaoxing University Scientific Research Project (Grant No. 20145030) for their financial support to the work present in this paper.

References

[1] Gursel A P, Maryman H, Ostertag C. A life-cycle approach to environmental, mechanical, and durability properties of “green” concrete mixes with rice husk ash. Journal of Cleaner Production, 2016, 112: 823-836.

[2] Johari M A M, Zeyad A M, Bunnori N M, et al. Engineering and transport properties of high-strength green concrete containing high volume of ultrafine palm oil fuel ash. Construction & Building Materials, 2012, 30(30): 281-288.

[3] Valipour M, Yekkalar M, Shekarchi M, et al. Environmental assessment of green

concrete containing natural zeolite on the global warming index in marine environments. Journal of Cleaner Production, 2014, 65(4): 418-423.

[4] Sheen Y N, Wang H Y, Sun T H. Properties of green concrete containing stainless steel oxidizing slag resource materials. Construction & Building Materials, 2014, 50(1): 22-27.

[5] Lothenbach B, Scrivener K, Hooton R D. Supplementary cementitious materials. Cement & Concrete Research, 2011, 41(3): 217-229.

[6] Aprianti E, Shafigh P, Bahri S, et al. Supplementary cementitious materials origin from agricultural wastes-A review. Construction & Building Materials, 2015, 74: 176–187.

[7] Snellings R, Mertens G, Elsen J. Supplementary cementitious materials. Reviews in Mineralogy & Geochemistry, 2012, 74(74): 211-278.

[8] Elahi A, Basheer P A M, Nanukuttan S V, et al. Mechanical and durability properties of high performance concretes containing supplementary cementitious materials. Construction & Building Materials, 2010, 24(3): 292-299.

[9] Meyer C. The greening of the concrete industry. Cement & Concrete Composites, 2009, 31(8): 601-605.

[10] Johari M A M, Brooks J J, Kabir S, et al. Influence of supplementary cementitious materials on engineering properties of high strength concrete. Construction & Building Materials, 2011, 25(5): 2639-2648.

[11] Sahmaran M, Yildirim G, Erdem T K. Self-healing capability of cementitious composites incorporating different supplementary cementitious materials. Cement &

Concrete Composites, 2013, 35(1): 89-101.

[12] Lei Z, Shuzhen Lv, Yong L, et al. Influence of lithium slag on cement properties. Journal of Wuhan University of Technology, 2015, 37(3): 23-27.

[13] Wu F F, Shi K B, Dong S K. Influence of concrete with lithium-slag and steel slag by early curing conditions. Key Engineering Materials, 2014, 599: 52-55.

[14] Wu F F, Shi K B, Dong S K. Properties and microstructure of HPC with lithium-slag and fly ash. Key Engineering Materials, 2014, 599: 70-73.

[15] Hongbo Tan, Xiangguo Li, Chao He, et al. Utilization of lithium slag as an admixture in blended cements: physico-mechanical and hydration characteristics. Journal of Wuhan University of Technology-Mater. Sci. Ed. 2015, 30(1): 129-133.

[16] Fufei Wu, Liangliang Chen, Kebin Shi, et al. Properties and microstructure of HPC with lithium-slag. Science Technology and Engineering, 2015, 15(12): 219-222.

[17] Lanfang Zhang. Experiment study on high-performance lithium-slag concrete. Journal of Liaoning Technical University, 2007, 26(6): 877-880.

[18] Kim J K, Sang H H, Song Y C. Effect of temperature and aging on the mechanical properties of concrete: Part I. Experimental results. Cement & Concrete Research, 2002, 32(7): 1087-1094.

[19] Sabir B B, Wild S, Bai J. Metakaolin and calcined clays as pozzolans for concrete: a review. Cement & Concrete Composites, 2001, 23(6): 441-454.

[20] Siddique R. Utilization of silica fume in concrete: Review of hardened properties. Resources Conservation & Recycling, 2011, 55(11): 923-932.

[21] He Z H, Li L Y, Du S G. Creep analysis of concrete containing rice husk ash.

Cement and Concrete Composites 2017, 80: 190-199.

[22] He Z H, Wu R Q, Yu Y F, Gao Y Q. Effect of Lithium Slag on Drying Shrinkage of Concrete with Manufactured-sand. Journal of Residuals Science & Technology, 2017, 14(1): 171-176.

[23] Diamond S. Mercury porosimetry: An inappropriate method for the measurement of pore size distributions in cement-based materials. Cement & Concrete Research, 2000, 30(10): 1517-1525.

[24] Gallé C. Effect of drying on cement-based materials pore structure as identified by mercury intrusion porosimetry: A comparative study between oven-, vacuum-, and freeze-drying. Cement & Concrete Research, 2001, 31(10): 1467-1477.